An Efficient Method for Small-Signal Stability Assessment of $P - f/Q - \dot{V}$ Droop Control in an Isolated Micro-Grid

Mohanraj Bellie Subramani, Srinivas Gude, Kuan-Chu Lin, and Chia-Chi Chu, *Senior Member, IEEE*

***Abstract*—An efficient method for small-signal stability assessment of $P - f/Q - \dot{V}$ droop control methods for multiple converters in an isolated micro-grid (MG) is proposed in this paper. A MG model described with arbitrary number of converters is explored first. If there are more number of converters in a chosen MG, only dominant eigenvalues related to droop control are of primary interest. Therefore, constructing a reduced-order model to speed up the small-signal stability assessment becomes necessary. By extending the previous work of MG with $P-f/Q-V$ droop control, a reduced-order model of MG with $P-f/Q-\dot{V}$ droop control is investigated under mild assumptions. Such a simplified model will facilitate to compute the poles and zeros of the closed-loop systems and provide more physical insight to examine the relationship between dominant eigenvalues and each droop control gain. As the mathematical analysis of conventional $P - f/Q - V$ droop control provides the characteristic polynomials contributed by $P - f$ and $Q - V$ droop controls, the $P - f/Q - \dot{V}$ droop control also provides a similar characteristic polynomials contributed by $P - f$ and $Q - \dot{V}$ droop controls. These characteristic polynomials of the system helps MG operators for better tuning of each droop gain for stable operation of MG. A detailed study of actual plant model and the reduced-order plant model are investigated. Both simulation and experimental results are presented to validate the proposed method.**

***Index Terms*—Micro-Grid (MG), Droop control, Power Converters, Small-Signal Stability, Characteristic Polynomials.**

I. Introduction

With recent advocates of distributed energy resources (DERs), the concept of micro-grid (MG) has been widely investigated recently as an effective way to integrate DERs into the existing AC power grid [1] - [3]. In order to achieve robust plug-and-play features, the MG can be operated either in the islanded mode or in the gridconnected mode. In the islanded mode, DERs interface power converters (DICs) in the MG are governed by droop control strategies for autonomous operations [3] - [12]. With the $P-f$ droop control, an accurate real power sharing can be obtained among the DICs. However, with $Q-V$ droop control, the reactive power sharing is highly dependent on DICs output filter and power cable impedances [13]. The autonomous load sharing with Q-V droop control can be affected by unequal filter and line impedances of DICs [14]- [15]. In order to resolve this difficulty, the $Q-\dot{V}$ droop control method has been proposed recently to improve the reactive power sharing among DICs [16]. Small-signal stability analysis of $P - f$ and $Q - \dot{V}$ is first explored in [16].

The precise eigenvalue analysis of the MG has been achieved and their results show that the dominant eigenvalues are due to droop control [17] - [18]. In [19] - [20], it has been found that, as the droop control gains of the MG increases the stability margin will decrease. In particular, for higher values of droop control gains, the closed-loop system becomes unstable. However, as there are more number of DICs in MG, only dominant eigenvalues related to the droop control are of primary interest. Under such condition, it is necessary to reduce the order of the MG plant model through mathematical analysis and find small signal stability of the reduced order plant model.

In order to lessen the computational complexity and provide more physical insight, a reduced-order modeling technique for the MG adopting the $P - f/Q - V$ droop control has been proposed in [21]. Under mild assumptions, it has been shown that the droop control gains of each DIC can be examined separately with corresponding characteristic polynomial equation. Thus dominant poles of the closed-loop system can be easily analyzed by the root locus technique. This method has provided more physical insight to examine the relationship between dominant eigenvalues and each droop gain.

In this paper, we extend the work of [21] by constructing the reduced-ordered dynamic model for a MG with $P-f/Q-\dot{V}$ droop control. As the mathematical analysis of conventional $P-f/Q-V$ droop control provides the characteristic polynomials contributed by $P - f$ and $Q - V$ droop controls, the $P - f/Q - \dot{V}$ droop control also provides a similar characteristic polynomials contributed by $P - f$ and $Q - \dot{V}$ droop controls. These characteristic polynomials of the system helps MG operators for better tuning of each droop gain for stable operation of MG. A detailed study of actual plant model and the reduced-order plant model are investigated.

The rest of this paper is organized as follows. In Section II, MG plant model in reduced order form has been derived for a chosen MG network structure. In Section III, the $P-f/Q-\dot{V}$ droop controller equations are brought to the convenient form to append the droop control equations in to open loop plant model derived in Section II. The reduced order plant model with $P-f/Q-\dot{V}$ droop control equations is derived to carry out small signal stability assessment of the system. Section IV,

This work was supported in part by the Ministry of Science and Technology, Taiwan, R.O.C., under Grant NSC 102-3113-P-002-037, NSC 103-ET-E-007-002-ET, MOST 103-2221-E-007-084, and MOST 103-3113-E-002-014. All authors contributed equally to this work.

The authors are with the Department of Electrical Engineering, National Tsing Hua University, Hsinchu, Taiwan, R.O.C., (e-mail: s104003894@m104.nthu.edu.tw; s103061880@m103.nthu.edu.tw; chire@kimo.com; ccchu@ee.nthu.edu.tw).

978-1-4799-8397-1/16/$31.00 © 2016 IEEE

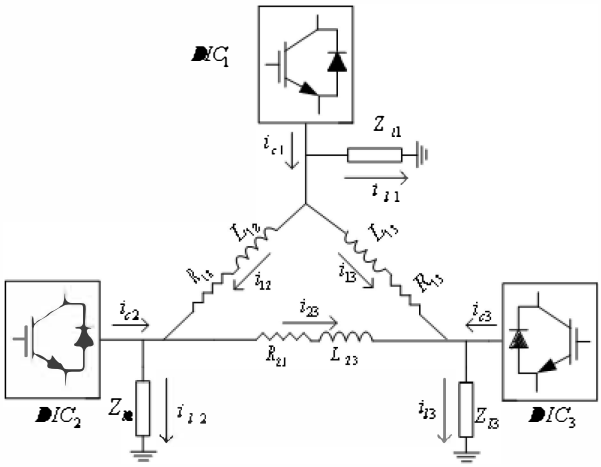

Fig. 1: Ring Connected Three DICs - MG structure

presents the simulation and experimental results of proposed system. Finally, some conclusions are made in Section V.

II. Open-Loop MG Model

In this section, we will follow [21]'s notion to construct the MG. The complete MG model without droop control will be considered first. Then, a reduced-order MG model without droop control will be derived. For illustration purpose, we consider the one-line diagram of a three-phase DIC MG as shown in Fig. 1. It consists of three DICs, each DIC consists of six IGBTs with anti-parallel diodes, fed with a constant DC voltage source. Each DIC consists of $L-C$ low-pass filter at the output to filter-out the higher order switching frequency components. The output voltage of each DIC is the voltage across capacitor C_f of the filter. All DICs are operated with space vector pulse width modulation (SVPWM) switching technique with current and voltage regulation. DIC_1, DIC_2 and DIC_3 have local balanced linear loads with impedances Z_{l1}, Z_{l2} and Z_{l3} respectively. Z_{12}, Z_{13} and Z_{23} are the cable impedances with resistances R_{12}, R_{13} and R_{23} and inductances L_{12}, L_{13} and L_{23} respectively.

A. Open-loop Plant Model

Since variations in amplitude and/or phase of phasor variables in MGs are slow enough in comparison with fast transient dynamics of power electronics, the pseudo steady state analysis is sufficient for modeling and analysis for MG droop control problems. It is assumed that all current and voltage variables are described in the synchronously rotating $d-q$ reference frame. Since the system considered is a balanced system, all variables in $d-q$ frame are DC-quantities under steady-state. Each transformed $d-q$ frame variable is expressed in real and imaginary complex variable. The following notations are considered for subsequent analysis: For $m=1,2$ and 3, $v_m = v_{md} + jv_{mq}$ is the output voltage of the DIC_m, $i_{cm} = i_{cmd} + ji_{cmq}$ is the output current of the DIC_m, $i_{lm} = i_{lmd} + ji_{lmq}$ is the local load current of the DIC_m, and $u_m = \theta_m - jV_m$ is the control signal input of the DIC_m. Line currents between the DICs are $i_{12} = i_{12d} + ji_{12q}$, $i_{13} = i_{13d} + ji_{13q}$ and $i_{23} = i_{23d} + ji_{23q}$. The angle θ_m is defined as follows [17]:

$$\theta_m = tan^{-1}(v_{mq}/v_{md}) \tag{1}$$

Since (1) is a non-linear equation, the following linearized form will be utilized for subsequent analysis:

$$\Delta\theta_m = (-V_{mq}\Delta v_{md} + V_{md}\Delta v_{mq})/(V_{md}^2 + V_{mq}^2) \tag{2}$$

The variable V_m denotes the output voltage magnitude of DIC_m defined by

$$V_m = \sqrt{(v_{md}^2 + v_{mq}^2)/(V_{md}^2 + V_{mq}^2)}. \tag{3}$$

Its linearized form can be written as:

$$\Delta V_m = (V_{mq}\Delta v_{md} + V_{md}\Delta v_{mq})/(V_{md}^2 + V_{mq}^2). \tag{4}$$

Thus, the complex variable u_m can be expressed in small-signal model as follows:

$$\Delta u_m = k_{um}\Delta v_m = (-V_{mq} - jV_{md})\Delta v_m/(V_{md}^2 + V_{mq}^2). \tag{5}$$

When all three DICs are considered, (5) can be expressed in the following matrix form:

$$\begin{bmatrix} -A_u & I \end{bmatrix} \begin{bmatrix} \Delta u \\ \Delta v \end{bmatrix} = 0, \tag{6}$$

where $A_u = \text{diag}[1/k_{u1}, 1/k_{u2}, 1/k_{u3}]$.
By applying load voltage equations, $\Delta v_m = Z_{lm}\Delta i_{lm}$, where $Z_{lm} = R_{lm} + sL_{lm} + j\omega L_{lm}$, we get the following matrix form:

$$\begin{bmatrix} -A_l & I \end{bmatrix} \begin{bmatrix} \Delta v \\ \Delta i_l \end{bmatrix} = 0, \tag{7}$$

where $A_l = \text{diag}[1/Z_{l1}, 1/Z_{l2}, 1/Z_{l3}]$.
Now by applying KCL at all nodes in Fig. 1, we have

$$\begin{bmatrix} I & -I & A_L \end{bmatrix} \begin{bmatrix} \Delta i_c \\ \Delta i_l \\ \Delta i_L \end{bmatrix} = 0, \tag{8}$$

where

$$A_L = \begin{bmatrix} -1 & 0 & -1 \\ 1 & -1 & 0 \\ 0 & 1 & 1 \end{bmatrix}.$$

Similarly, by applying KVL for three branches with impedances Z_{12}, Z_{13} and Z_{23}, we have:

$$\begin{bmatrix} -A_z & I \end{bmatrix} \begin{bmatrix} \Delta v \\ \Delta i_L \end{bmatrix} = 0 \tag{9}$$

where,

$$A_z = \begin{bmatrix} \frac{1}{Z_{l2}} & -\frac{1}{Z_{l2}} & 0 \\ 0 & \frac{1}{Z_{23}} & -\frac{1}{Z_{23}} \\ \frac{1}{Z_{l3}} & 0 & -\frac{1}{Z_{l3}} \end{bmatrix},$$

where $Z_{mn} = R_{mn} + sL_{mn} + j\omega L_{mn}$ for $m, n = 1, 2$ and 3, such that $m \neq n$.

Now, by combining (6)–(9), the complete open-loop plant model of the MG system can be expressed as:

$$[A][\Delta x] = 0 \tag{10}$$

$$\begin{bmatrix} -A_u & I & 0 & 0 & 0 \\ 0 & 0 & I & -I & A_L \\ 0 & -A_l & 0 & I & 0 \\ 0 & -A_z & 0 & 0 & I \end{bmatrix} \begin{bmatrix} \Delta u \\ \Delta v \\ \Delta i_c \\ \Delta i_l \\ \Delta i_L \end{bmatrix} = 0 \qquad (11)$$

B. Reduced-Order Model

Equation (11) is the complete open-loop plant model of the MG without considering the droop control. However, the order of the closed-loop plant model will become extremely high as the number of DIC's increase for practical industrial applications. In order to reduce the computational complexity, the order of the plant model needs to be reduced by eliminating variables which does not affect the droop control equations significantly. This task can be achieved by pre-multiplying a uni-modular matrix $[U]$ with matrix $[A]$. Since $|U| = 1$, the unimodular matrix $[U]$ is chosen as

$$[U] = \begin{bmatrix} I & 0 & 0 & 0 \\ (A_l - A_L A_z) & I & I & -A_L \\ 0 & 0 & I & 0 \\ 0 & 0 & 0 & I \end{bmatrix}, \qquad (12)$$

and

$$[U][A] = \begin{bmatrix} -A_u & I & 0 & 0 & 0 \\ -(A_l - A_L A_z)A_u & 0 & I & 0 & 0 \\ 0 & -A_l & 0 & I & 0 \\ 0 & A_z & 0 & 0 & I \end{bmatrix}. \qquad (13)$$

Now consider the droop dynamics. Since only the output voltage Δv_m and the output current Δi_{cm} of each DIC are considered for implementing the feedback decentralized droop control loop, each droop controller can be implemented as two-input and one-output linear system of the form: for $m = 1, 2, 3$

$$-C_{imp_m} u_m = C_{v_m} \Delta v_m + C_{ic_m} \Delta i_{cm}.$$

where C_{v_m} and C_{ic_m} define the denominator of the droop control transfer function from the output voltage Δv_m and the output current Δi_{cm} respectively. C_{imp_m} is the numerator of the droop control transfer function to control input u. Analytical expressions of C_{v_m}, C_{ic_m}, and C_{imp_m} will derived in the next section. If we define $C_{imp} = \text{diag}[C_{imp_1}, C_{imp_2}, C_{imp_3}]$, $C_v = \text{diag}[C_{v_1}, C_{v_2}, C_{v_3}]$, and $C_{ic} = \text{diag}[C_{ic_1}, C_{ic_2}, C_{ic_3}]$, the droop control can be expressed in the following block matrix form as:

$$C\Delta x = \begin{bmatrix} C_{imp} & C_v & C_{ic} & 0 & 0 \end{bmatrix} \Delta x = 0. \qquad (14)$$

If these droop controller coefficients are appended to the matrix in (13), the closed-loop MG plant model is formed as follows:

$$[A_{closed}][\Delta x] = 0, \qquad (15)$$

where

$$A_{closed} = \left[\begin{array}{ccc|cc} -A_u & I & 0 & 0 & 0 \\ -(A_l - A_L A_z)A_u & 0 & I & 0 & 0 \\ C_{imp} & C_v & C_{ic} & 0 & 0 \\ \hline 0 & -A_l & 0 & I & 0 \\ 0 & A_z & 0 & 0 & I \end{array}\right] \qquad (16)$$

The determinant of A_{closed} provides the characteristic polynomial of the closed-loop system, so that the stability can be analyzed. Since the matrix A_{closed} is of higher order, the determinant of the A_{closed} can be examined by its corresponding Schur's complement as,

$$|A_{closed}| = \begin{vmatrix} -A_u & I & 0 \\ -(A_l - A_L A_z)A_u & 0 & I \\ C_{imp} & C_v & C_{ic} \end{vmatrix}, \qquad (17)$$

where

$$(A_l - A_L A_z) = \begin{bmatrix} \frac{1}{Z_{l1}} + \frac{1}{Z_{12}} + \frac{1}{Z_{13}} & -\frac{1}{Z_{12}} & -\frac{1}{Z_{13}} \\ -\frac{1}{Z_{12}} & \frac{1}{Z_{l2}} + \frac{1}{Z_{12}} + \frac{1}{Z_{23}} & -\frac{1}{Z_{23}} \\ -\frac{1}{Z_{13}} & -\frac{1}{Z_{23}} & \frac{1}{Z_{l3}} + \frac{1}{Z_{13}} + \frac{1}{Z_{23}} \end{bmatrix}.$$

Since the load impedance is much larger than each line impedance between DICs, Z_l terms can be neglected in $(A_l - A_L A_z)$. Thus, $(A_l - A_L A_z)$ can be simplified as

$$A_l - A_L A_z = \begin{bmatrix} \frac{1}{Z_{l2}} + \frac{1}{Z_{l3}} & -\frac{1}{Z_{l2}} & -\frac{1}{Z_{l3}} \\ -\frac{1}{Z_{l2}} & \frac{1}{Z_{l2}} + \frac{1}{Z_{23}} & -\frac{1}{Z_{23}} \\ -\frac{1}{Z_{l3}} & -\frac{1}{Z_{23}} & \frac{1}{Z_{l2}} + \frac{1}{Z_{l2}} \end{bmatrix}.$$

III. Reduced-Order Plant Model with $P - f/Q - \dot{V}$ Droop Control

In this section, first $P-f/Q-\dot{V}$ droop control equations are brought to the convenient form to append the equations to the open loop plant model derived in Section II and then reduced order model with $P - f/Q - \dot{V}$ droop control is derived.

A. Droop Control Mechanism

The $P - f/Q - \dot{V}$ droop control with voltage restorations can be described as follows: for $m = 1, 2, 3$,

$$\omega_m = s\theta_m = \omega_0 - k_{pm}(p_m - p_{0m}), \qquad (18a)$$
$$\dot{V}_m = sV_m = \dot{V}_0 - k_{qm}(q_m - q_{0m}), \qquad (18b)$$
$$\dot{Q}_{0m} = sq_{0m} = K_{res}Q_{rm}(\dot{V}_{0m} - \dot{V}_m), \qquad (18c)$$

where ω_m is the angular frequency of converter output voltage; ω_0 is the nominal grid frequency; V_m is the magnitude of the converter output voltage; $\dot{V}_{0m}$ is the nominal value of $\dot{V}_m$; p_m is the active power generated by the converters; p_{0m} is the nominal active power; q_{0m} is the reactive power; k_{pm} is the droop control gain for $P - f$ droop control; k_{qm} is the droop control gain for $Q - \dot{V}$ droop control; K_{res} is the $\dot{V}$ restoration gain; Q_{rm} is the rated reactive power capacity. p_m and q_m can be expressed analytically as

$$p_m = v_{md}i_{cmd} + v_{mq}i_{cmq} \qquad (19a)$$
$$q_m = v_{mq}i_{cmd} - v_{md}i_{cmq} \qquad (19b)$$

By linearizing (19), we have

$$\Delta p_m = I_{cmd}\Delta v_{md} + I_{cmq}\Delta v_{mq} + V_{md}\Delta i_{cmd} + V_{mq}\Delta i_{cmq} \qquad (20a)$$
$$\Delta q_m = I_{cmd}\Delta v_{mq} - I_{cmq}\Delta v_{md} + V_{mq}\Delta i_{cmd} - V_{md}\Delta i_{cmq} \qquad (20b)$$

I_{cmd} and I_{cmq} are the values of i_{cmd} and i_{cmq} output currents of converter m respectively. At an equilibrium point, the linearized droop control equations can be described as:

$$s\Delta\theta = -k_{pm}\Delta p_m \qquad (21a)$$
$$s\Delta V_m = -k_{qm}\Delta q_m + k_{qm}\Delta q_{0m} \qquad (21b)$$
$$(s + k_{qm}K_{res}Q_{rm})\Delta q_{0m} = k_{qm}K_{res}Q_{rm}\Delta q_m \qquad (21c)$$

By substituting terms Δp_m and Δq_m obtained in (20) into the linearized droop control equations in (21), we have

$$s\Delta\theta_m = -k_{pm}(I_{cmd}\Delta v_{md} + I_{cmq}\Delta v_{mq} + V_{md}\Delta i_{cmd} + V_{mq}\Delta i_{cmq}) \quad (22a)$$

$$s\Delta V_m = k_{qm}(I_{cmq}\Delta v_{md} - I_{cmd}\Delta v_{mq} - V_{mq}\Delta i_{cmd} + V_{md}\Delta i_{cmq}) + k_{qm}\Delta q_{0m} \quad (22b)$$

$$(s + k_{qm}K_{res}Q_{rm})\Delta q_{0m} = -k_{qm}K_{res}Q_{rm}(I_{cmq}\Delta v_{md} - I_{cmd}\Delta v_{mq} - V_{mq}\Delta i_{cmd} + V_{md}\Delta i_{cmq}) \quad (22c)$$

The droop control for m DICs can be generalized and can be represented in the following matrix form:

$$\begin{bmatrix} sI \\ 0 \\ 0 \end{bmatrix}\Delta\theta_m + \begin{bmatrix} 0 \\ sI \\ 0 \end{bmatrix}\Delta V_m + \begin{bmatrix} 0 \\ E \\ E_1 \end{bmatrix}\Delta q_{0m} + \begin{bmatrix} C_{vd} \\ D_{vd} \\ E_2 \end{bmatrix}\Delta v_{md} + \begin{bmatrix} C_{vq} \\ D_{vq} \\ E_3 \end{bmatrix}\Delta v_{mq} + \begin{bmatrix} C_{id} \\ D_{id} \\ E_4 \end{bmatrix}\Delta i_{cmd} + \begin{bmatrix} C_{iq} \\ D_{iq} \\ E_5 \end{bmatrix}\Delta i_{cmq} = 0, \quad (23)$$

where

$$\begin{aligned} E &= diag(k_{qm}), \\ E_1 &= SI + diag(k_{qm})K_{res}Q_{rm}, \\ E_2 &= D_{vd}K_{res}Q_{rm}, \\ E_3 &= D_{vq}K_{res}Q_{rm}, \\ E_4 &= D_{id}K_{res}Q_{rm}, \\ E_5 &= D_{iq}K_{res}Q_{rm}, \\ \theta &= \begin{bmatrix}\theta_1 & \theta_2 & \theta_3\end{bmatrix}, \\ V_m &= \begin{bmatrix}-V_1 & -V_2 & -V_3\end{bmatrix}, \\ q_{0m} &= \begin{bmatrix}q_{01} & q_{02} & q_{03}\end{bmatrix}, \\ v_{md} &= \begin{bmatrix}v_{1d} & v_{2d} & v_{3d}\end{bmatrix}, \\ v_{mq} &= \begin{bmatrix}v_{1q} & v_{2q} & v_{3q}\end{bmatrix}, \\ i_{cmd} &= \begin{bmatrix}i_{c1d} & i_{c2d} & i_{c3d}\end{bmatrix}, \\ i_{cmq} &= \begin{bmatrix}i_{c1q} & i_{c2q} & i_{c3q}\end{bmatrix}, \\ k_{pm} &= \begin{bmatrix}k_{p1} & k_{p2} & k_{p3}\end{bmatrix}, \\ k_{qm} &= \begin{bmatrix}k_{q1} & k_{q2} & k_{q3}\end{bmatrix}, \\ C_{vd} &= \left[diag(k_{pm}) \times diag(I_{cmd})\right], \\ C_{vq} &= \left[diag(k_{pm}) \times diag(I_{cmq})\right], \\ C_{id} &= \left[diag(k_{pm}) \times diag(V_{md})\right], \\ C_{iq} &= \left[diag(k_{pm}) \times diag(V_{mq})\right], \\ D_{vd} &= \left[diag(k_{qm}) \times diag(I_{cmq})\right], \\ D_{vq} &= \left[-diag(k_{qm}) \times diag(I_{cmd})\right], \\ D_{id} &= \left[-diag(k_{qm}) \times diag(V_{mq})\right], \\ D_{iq} &= \left[diag(k_{qm}) \times diag(V_{md})\right]. \end{aligned}$$

Note that V_m is chosen as negative sign to remain in accordance with the definition of $u_m = \theta_m - jV_m$. Taking one matrix as example: $C_{vq} = \text{diag}[k_{p1}I_{c1q}, k_{p2}I_{c2}, k_{p3}I_{c3}]$. The Matrices $C_{vd}, C_{vq}, C_{id}, C_{iq}, D_{vd}, D_{vq}, D_{id}$ and D_{iq} are defined in a similar form.

B. Reduced-Order Model with $P - f/Q - \dot{V}$ Droop Control

To obtain the reduced-order model with $P-f/Q-\dot{V}$ droop control, the reduced-order plant model equations obtained in (17) are appended with the droop controller equations derived in (23). Henceforth, the following matrix representation can be obtained:

$$[A_{cl}][\Delta x] = 0 \quad (24)$$

where

$$A_{cl} = \begin{bmatrix} -A_u^r & A_u^i & 0 & I & 0 & 0 & 0 \\ -A_u^i & -A_u^r & 0 & 0 & I & 0 & 0 \\ -A_{imp}^r & A_{imp}^i & 0 & 0 & 0 & I & 0 \\ -A_{imp}^i & -A_{imp}^r & 0 & 0 & 0 & 0 & I \\ sI & 0 & 0 & C_{vd} & C_{vq} & C_{id} & C_{iq} \\ 0 & sI & E & D_{vd} & D_{vq} & D_{id} & D_{iq} \\ 0 & 0 & E_1 & E_2 & E_3 & E_4 & E_5 \end{bmatrix}$$

and

$$\Delta x = \left[\Delta\theta, \Delta V, \Delta q_{0m}, \Delta v_{md}, \Delta v_{mq}, \Delta i_{cmd}, \Delta i_{cmq}\right]^T$$

and $A_{imp} = (A_l - A_L A_z)A_u$. Note that A_u can be expressed in complex real and imaginary components as A_u^r and A_u^i respectively. Similarly, A_{imp} can be expressed in complex real and imaginary components as A_{imp}^r and A_{imp}^i respectively.

The determinant of A_{cl} gives the characteristic polynomial of the closed-loop system. In order to reduce the computational complexity, the order reduction techniques developed in Section II is applied once again for matrix A_{cl}. Let matrix A_{cl} be pre-multiplied by a uni-modular matrix U defined by

$$U_{cl} = \begin{bmatrix} I & 0 & 0 & 0 & 0 & 0 & 0 \\ 0 & I & 0 & 0 & 0 & 0 & 0 \\ 0 & 0 & I & 0 & 0 & 0 & 0 \\ 0 & 0 & 0 & I & 0 & 0 & 0 \\ -C_{vd} & -C_{vq} & -C_{id} & -C_{iq} & I & 0 & 0 \\ -D_{vd} & -D_{vq} & -D_{id} & -D_{iq} & 0 & I & 0 \\ -E_2 & -E_3 & -E_4 & -E_5 & 0 & 0 & I \end{bmatrix},$$

the product $U_{cl}A_{cl}$ becomes

$$U_{cl}A_{cl} = \left[\begin{array}{ccc|cccc} -A_u^r & A_u^i & 0 & I & 0 & 0 & 0 \\ -A_u^i & -A_u^r & 0 & 0 & I & 0 & 0 \\ -A_{imp}^r & A_{imp}^i & 0 & 0 & 0 & I & 0 \\ -A_{imp}^i & -A_{imp}^r & 0 & 0 & 0 & 0 & I \\ \hline C_\delta^{mod} & C_V^{mod} & 0 & 0 & 0 & 0 & 0 \\ D_\delta^{mod} & D_V^{mod} & E & 0 & 0 & 0 & 0 \\ D_{res1}^{mod} & D_{res2}^{mod} & E_1 & 0 & 0 & 0 & 0 \end{array}\right] \quad (25)$$

where,

$$\begin{aligned} C_\delta^{mod} &= sI + C_{vd}A_u^r + C_{vq}A_u^i + C_{id}A_{imp}^r + C_{iq}A_{imp}^i, \\ C_V^{mod} &= -C_{vd}A_u^i + C_{vq}A_u^r - C_{id}A_{imp}^t + C_{iq}A_{imp}^r, \\ D_\delta^{mod} &= D_{vd}A_u^r + D_{vq}A_u^i + D_{id}A_{imp}^r + D_{iq}A_{imp}^t, \\ D_V^{mod} &= sI - D_{vd}A_u^i + D_{vq}A_u^r - D_{id}A_{imp}^i + D_{iq}A_{imp}^r, \\ D_{res1}^{mod} &= K_{res}Q_{rm}(-D_{vd}A_u^r + D_{vq}A_u^i + D_{id}A_{imp}^r + D_{iq}A_{imp}^i), \\ D_{res2}^{mod} &= K_{res}Q_{rm}(-D_{vd}A_u^i + D_{vq}A_u^r - D_{id}A_{imp}^i + D_{iq}A_{imp}^r). \end{aligned}$$

By Schurs complement, we have

$$|A_{cl}| = \begin{vmatrix} C_\delta^{mod} & C_V^{mod} & 0 \\ D_\delta^{mod} & D_V^{mod} & E \\ D_{res1}^{mod} & D_{res2}^{mod} & E_1 \end{vmatrix}. \quad (26)$$

$|A_{cl}|$ can be further simplified if the following three assumptions are made:

1) The output voltage phase angle difference between the DICs is small.
2) The output voltage magnitude difference between the DICs is very small.
3) At an equilibrium point chosen, $V_{1d} \approx V_{2d} \approx V_{3d}$=:$V_d$. and $V_{1q} \approx V_{2q} \approx V_{3q}$=:$V_q$.

Under these three assumptions, matrices

$C_\delta^{mod}, C_V^{mod}, D_\delta^{mod}, D_V^{mod}, D_{res1}^{mod}$ and D_{res2}^{mod} are simplified as follows:

1) $C_\delta^{mod} = sI + \text{diag}(k_{pm})[-Q + (V_d^2 + V_q^2)X]$, where $Q = \text{diag}(Q_1, Q_2, Q_3)$ and

$$X = \begin{bmatrix} X_{12}+X_{13} & -X_{12} & -X_{13} \\ -X_{12} & X_{12}+X_{23} & -X_{23} \\ -X_{13} & -X_{23} & X_{13}+X_{23} \end{bmatrix}.$$

$X_{mn} = \omega L_{mn}/|Z_{mn}|^2$ and $|Z_{mn}|^2 = (R_{mn} + sL_{mn})^2 + (\omega L_{mn})^2$.

2) $C_V^{mod} = \text{diag}(k_{pm})[-P - (V_d^2 + V_q^2)Y]$, where $P = \text{diag}[P_1, P_2, P_3]$ and

$$Y = \begin{bmatrix} Y_{12}+Y_{13} & -Y_{12} & -Y_{13} \\ -Y_{12} & Y_{12}+Y_{23} & -Y_{23} \\ -Y_{13} & -Y_{23} & Y_{13}+Y_{23} \end{bmatrix}.$$

$Y_{mn} = (R_{mn} + sL_{mn})/|Z_{mn}|^2$.

3) $D_\delta^{mod} = \text{diag}(k_{qm})[-P + (V_d^2 + V_q^2)Y]$.
4) $D_V^{mod} = sI + \text{diag}(k_{qm})[Q + (V_d^2 + V_q^2)X]$.
5) $D_{res1}^{mod} = K_{res}Q_{rm}\text{diag}(k_{qm})[-P + (V_d^2 + V_q^2)Y]$.
6) $D_{res2}^{mod} = K_{res}Q_{rm}\text{diag}(k_{qm})[Q + (V_d^2 + V_q^2)X]$

The variable ω represents the value of the angular frequency of the MG at the operating point when the frequencies of all DICs become equal. Usually, the variation of the frequency ω is sufficiently small if P-f droop control is activated, $\omega \approx \omega_0$. Similarly, the variation of the output voltage magnitude is also sufficiently small if $Q - \dot{V}$ droop control is activated, $(V_d^2 + V_q^2) \approx V_0^2$, where V_0 be the rated voltage of the system.

Since elements of matrix (25) are simplified, the determinant of A_{cl} can also be simplified. Since droop gains k_{pm} and k_{qm} are quite small, two or more products of such terms are very small and can be neglected. Thus, only the product of the diagonal terms in A_{cl} would contribute for the determiant of A_{cl}, since other terms have a product of two or more droop gains. Under this situation,

$$\begin{aligned} |A_{cl}| &\approx (C_\delta^{mod})(D_V^{mod})E_1 \\ &\approx (C_\delta^{mod})(D_V^{mod})(sI + diag(k_{qm})K_{res}Q_{rm}) \\ &\approx |(sI)[sI + diag(k_{pm})(-Q + V_0^2 X)] \\ &\quad \times [sI + diag(k_{qm})(K_{res}Q_{rm} + Q + V_0^2 X)]| \end{aligned} \quad (27)$$

If three DICs are considered, the characteristic polynomial for the closed-loop MG system can be expressed as

$$\begin{aligned} |A_{cl}| = s^3 &\times \left[s + k_{p1}(-Q_1 + V_0^2 \tfrac{\omega L_{12}}{|Z_{12}|^2} + V_0^2 \tfrac{\omega L_{13}}{|Z_{13}|^2}\right] \\ &\times \left[s + k_{p2}(-Q_2 + V_0^2 \tfrac{\omega L_{12}}{|Z_{12}|^2} + V_0^2 \tfrac{\omega L_{23}}{|Z_{23}|^2}\right] \\ &\times \left[s + k_{p3}(-Q_3 + V_0^2 \tfrac{\omega L_{13}}{|Z_{13}|^2} + V_0^2 \tfrac{\omega L_{23}}{|Z_{23}|^2}\right] \\ &\times \left[s + k_{q1}(K_{res}Q_{rm} + Q_1 + V_0^2 \tfrac{\omega L_{12}}{|Z_{12}|^2} + V_0^2 \tfrac{\omega L_{13}}{|Z_{13}|^2}\right] \\ &\times \left[s + k_{q2}(K_{res}Q_{rm} + Q_2 + V_0^2 \tfrac{\omega L_{12}}{|Z_{12}|^2} + V_0^2 \tfrac{\omega L_{23}}{|Z_{23}|^2}\right] \\ &\times \left[s + k_{q3}(K_{res}Q_{rm} + Q_3 + V_0^2 \tfrac{\omega L_{13}}{|Z_{13}|^2} + V_0^2 \tfrac{\omega L_{23}}{|Z_{23}|^2}\right] \end{aligned} \quad (28)$$

The effect of each individual droop gain can be examined through examining each polynomial in $|A_{cl}| = 0$. Each DIC appears to be transformed into an equivalent network with the interconnecting impedances connecting it to other DICs taken into account. The droop control are then applied to this equivalent network providing two polynomials for each DIC, one for P-f droop and the other for Q-$\dot{V}$ droop. The polynomial s corresponds to the action of time-derivative respect to V. Therefore, the small-signal stability of the closed-loop system can be examined by examining each polynomial independently with a single droop coefficient. For example, consider the following polynomial:

$$[s + k_{p1}(-Q_1 + V_0^2 \omega L_{12}/|Z_{12}|^2 + V_0^2 \omega L_{13}/|Z_{13}|^2)] = 0$$

which relates one dominate pole of the closed-loop system with respect to the P-f droop gain of the first DIC. The above equation can also be rewritten as

$$\begin{aligned} s|Z_{12}|^2|Z_{13}|^2 + k_{p1}(-Q_1|Z_{12}|^2|Z_{13}|^2 + \\ V_0^2 \omega L_{12}|Z_{13}|^2 + V_0^2 \omega L_{13}|Z_{12}|^2) = 0, \end{aligned} \quad (29)$$

which is expressed in the standard root locus form $den(s) + k.num(s) = 0$ of closed-loop system. $den(s)/num(s)$ is open loop transfer function.

Since the computational complexity of evaluating a single polynomial is far lesser than the computation of the determinant of the entire system model, the computational speed has been enhanced significantly. Thus, in order to ensure stable operation of all DICs for a chosen MG, a common k_p and k_q limit values can be found such that all the six polynomials in (28) are satisfied simultaneously.

If we compare the characteristic polynomial of the closed-loop system of the proposed $P - f/Q - \dot{V}$ droop control with the conventional $P - f/Q - V$ droop control, some observations can be made.

- Individual real-power droop characteristic polynomials have identical formulation in both droop controllers since both methods use same P-f droop control law. However, the reactive power droop characteristic polynomials are different from each other, since both methods use different reactive power droop control law.
- If $P-f/Q-\dot{V}$ droop control is applied, the characteristic polynomials of the closed loop system contributed by $P-f$ and $Q-\dot{V}$ droop controls have the same number with that of $P - f/Q - V$ droop control. This means that both real power droop and reactive power droop play a dual role in the droop control. This subtle property will facilitate tuning the droop gain.

IV. Simulation and Experimental Results

In order to verify the analytical results developed in the previous section, both simulation and experimental results of a MG with $P - f/Q - \dot{V}$ droop controlled DICs will be presented in this section. For illustration purpose, a MG with two DICs and a load, as shown in Fig.2, is studied. Simulink/MATLAB simulations are provided to show the movement of poles of the controlled system for varying droop gains. Hardware experimental results are reported to show the transient response of the proposed $P-f/Q-\dot{V}$ droop control. The system parameters are listed in Table I.

A. Simulation Results

Since only two DICs are considered in this example, only four polynomials will appear in the characteristic polynomial

TABLE I: Parameters of Hardware System

Parameter	Value
DIC rated power	1kW
DIC terminal voltage	110 V_{L-L}(rms)
System frequency, f	60 Hz
Inductance of DIC filter	2 mH
Capacitance of DIC filter	10 μF
Load resistance, R	12 ohm
Load inductance, L	30 mH
Resistance of transmission line, R_{23}	0.25 ohm
Inductance of Transmission line, L_{23}	2 mH
DC bus voltage, V_{DC}	400V

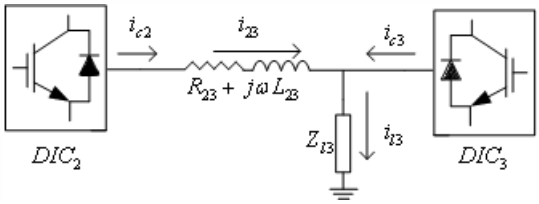

Fig. 2: The MG for experimental study

as shown below:

$$|A_{cl}| = s^3 \times G_{pf2}(s) \times G_{pf3}(s) \times G_{Qv2}(s) \times G_{Qv3}(s) \quad (30)$$

The closed-loop system stability is decided by the stability of each individual polynomial.

The polynomials $G_{pf2}(s)$, $G_{pf3}(s)$, $G_{Qv2}(s)$ and $G_{Qv3}(s)$ contain the gains k_{p2}, k_{p3}, k_{q2} and k_{q3} respectively. Table II lists expression for each polynomial and their corresponding zeros and poles. When the roots of the polynomials are plotted for varying positive droop gains, as per theory of root locus plots, the loci originate from the poles for zero gain and terminate at the zeros as gain tends to infinity.

Figures 3 - 6 shows the movement of roots of each polynomial as their respective control gains are varied. The arrows indicate the direction of movement of the roots as the control gains increases. In all the plots, the roots move into the right half of the s-plane for large values of the control gain. The zero on the right half of s-plane implies that the controlled system is unstable for large gains with root loci moving closer towards it. The value of the control gains $k_{p2} = k_{p3} = k_p$ and $k_{q2} = k_{q3} = k_q$ for which the controlled system becomes unstable is found to be $6.5 \times 10^{-3}(rad/(Ws))$ and $6.5 \times 10^{-3}(V/(VAR.s))$ respectively. If the control gains are smaller than above mentioned values, the controlled system is stable, as the roots are on the left side of the imaginary axis.

B. Experimental Results

We provide a hardware prototype platform to verify above mentioned simulation results. The parameters of the hardware experiment are listed in Table I. This hardware experiment is proceeded by the following two steps:

- DIC_3 is started with its drop controller and it generates output 110V (RMS (L-L), 60 Hz) to the load. During this step, DIC_2 is only locking the phase of the voltage output from DIC_3 but does not generate the power.

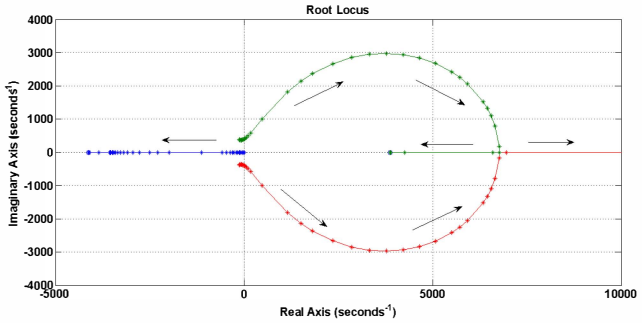

Fig. 3: Root locus of $G_{pf2}(s)$

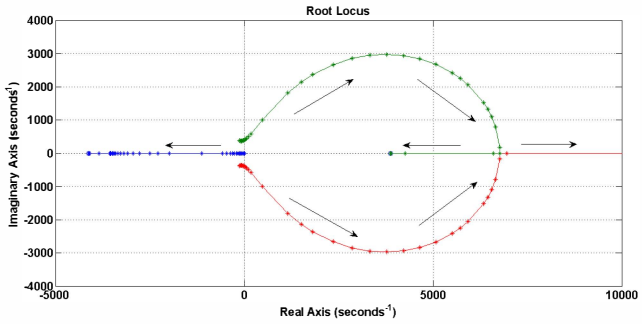

Fig. 4: Root Locus of $G_{pf3}(s)$.

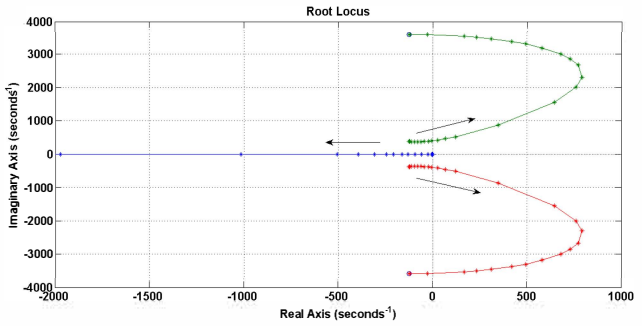

Fig. 5: Root locus of $G_{QV2}(s)$.

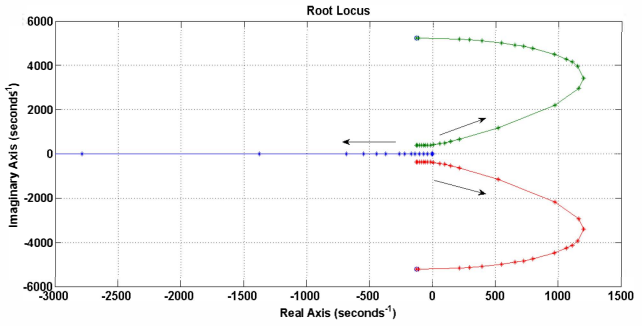

Fig. 6: Root Locus of $G_{QV3}(s)$.

TABLE II: Zeros and Poles of the Polynomials

Polynomial	Zeros	Poles
$G_{pf2}(s) = [s\|Z_{23}\|^2 + k_{p2}(-Q_2\|Z_{23}\|^2 + {V_0}^2\omega L_{23})]$	$-6480.4, 6230.4$	$-125 \pm j377, 0$
$G_{pf3}(s) = [s\|Z_{23}\|^2 + k_{p3}(-Q_3\|Z_{23}\|^2 + {V_0}^2\omega L_{23})]$	$-7069.5, 6819.5$	$-125 \pm j377, 0$
$G_{Q\dot{v}2}(s) = [s\|Z_{23}\|^2 + k_{q2}(K_{res}Q_{rm}\|Z_{23}\|^2 + Q_2\|Z_{23}\|^2 + {V_0}^2\omega L_{23})]$	$-125 \pm j3589$	$-125 \pm j377, 0$
$G_{Q\dot{v}3}(s) = [s\|Z_{23}\|^2 + k_{q3}(K_{res}Q_{rm}\|Z_{23}\|^2 + Q_3\|Z_{23}\|^2 + {V_0}^2\omega L_{23}\|Z_{13}\|^2)]$	$-125 \pm j5204$	$-125 \pm j377, 0$
s^3	–	$0, 0, 0$

TABLE III: Control gains of two cases

Control gain	Case 1	Case 2
$k_p(rad/(W.s))$	1×10^{-5}	1×10^{-5}
$k_q(V/(VAR.s))$	1×10^{-4}	1×10^{-3}

- DIC_2 is started with its droop controller and it generates output 110V (RMS (L-L), 60 Hz) to share its power along with DIC_3 to the load.

In order to verify the control gain values obtained by root locus method, two cases of different control gains are chosen as tabulated in Table III. Since paramters of two DICs are identical, droop control gains are set as $k_{p2} = k_{p3} = k_p$ and $k_{q2} = k_{q3} = k_q$.

The experimental results in Figures 7 - 10 show the corresponding active power and the reactive power outputs of two DICs. From Figure 7 and 8, it is clear that the $P - f/Q - \dot{V}$ droop control method is feasible for regulating the power sharing between two DICs in practice. At first, the active power and the reactive power is supported by DIC_3 solely and DIC_2 does not generate any power. When the droop control for DIC_2 is enabled, DIC_2 starts generating power and the power outputs of the two DICs are redistributed.

In case 1, as the control gains are small enough, the two DICs share active power evenly under steady-state (approximately 267 Watts). Since restoration mechanism for the term $\dot{V}$ is applied, the reactive power is not been shared evenly by the two DICs under steady-state ($DIC_3 = 377.4VAR$, $DIC_2 = 125.7VAR$). In case 2, as one of the control gain k_q is nearer to the value of 6.5×10^{-3}, it is to find that the power sharing between the two DICs has weak damping behavior. This weak damping behaviour indicates that the roots are very nearer to the imaginary axis of the complex plane.

V. Conclusion

In this paper, a model for multiple DICs connected in a MG is presented first. An efficient method for constructing a reduced order MG has been extended for DICs with $P - f/Q - \dot{V}$ droop control. The closed-loop transfer function characteristic equation is obtained under mild assumptions and this the poles and zeros of the plant model are be obtained. These line impedances between the DICs and droop control gains produce a high impact on the location of poles and zeros on the complex plane and thereby the stability of the entire system. The root locus method is explored for proper tuning of the droop gains. By observing root locus of varied control

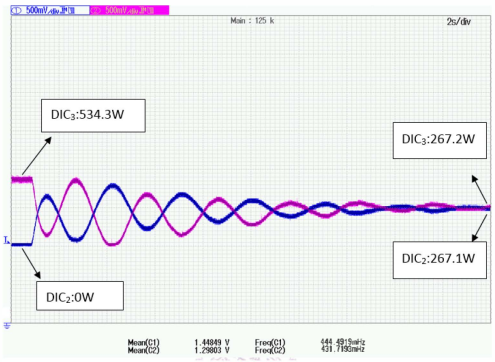

Fig. 7: Active power sharing between two DICs in Case 1.

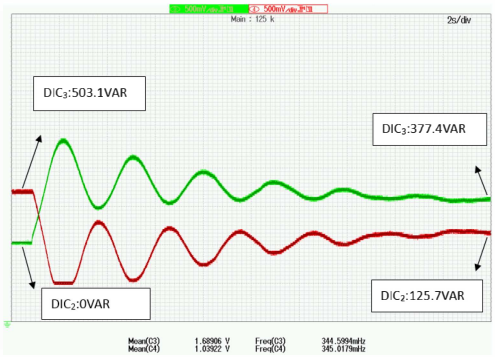

Fig. 8: Reactive power sharing between two DICs in Case 1.

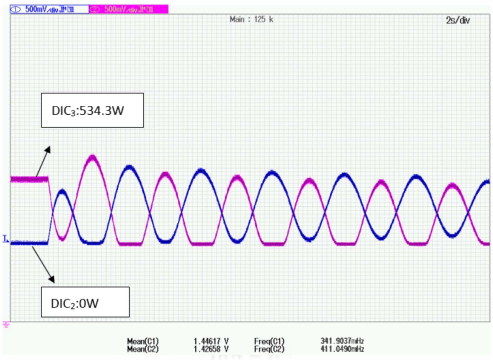

Fig. 9: Active power sharing between two DICs in Case 2.

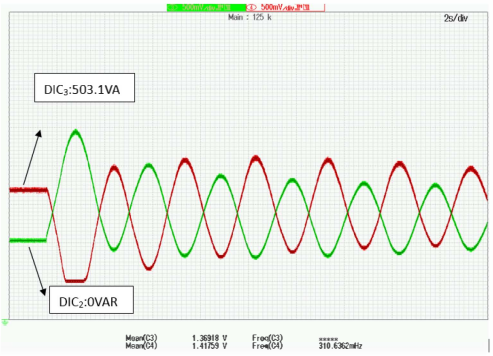

Fig. 10: Reactive power sharing between two DICs in Case 2.

gains, the stability limits of the plant model are examined. Both simulation studies and experimental results show the correctness of the proposed analysis.

REFERENCES

[1] R. Lasseter, "Mirogirds," *in Proc. IEEE Power Eng. Soc. Winter Meet.*, 2002, pp. 305-308.

[2] M. Barnes, J. Kondoh, H. Asano, J. Oyarzabal, G. Ventakaramanan, R. Lasseter, N. Hatziargyriou, and T. Green, "Real-world Microgrids-an overview," *in Proc. IEEE Int. Conf. Syst. Syst. Eng.*, Apr., 2007, pp. 1-8.

[3] R. H. Lasseter, J. H. Eto, B. Schenkman, J. Stevens, H. Vollkommer, D. Klapp, E. Linton, H. Hurtado, and J. Roy, "Certs Microgrid laboratory test bed," *IEEE Trans. Power Del.*, vol. 26, no. 1, pp. 325332, Jan. 2011.

[4] M. C. Chandrokar, D. M. Divan, and R. Adapa, "Control of parallel connected inverters in standalone ac supply systems," *IEEE Trans. Ind. Appl.*, vol. 29, no. 1, pp. 136-143, Jan./Feb. 1993.

[5] P. Piagi and R. Lasseter,"Autonomous control of Microgrids," *in Proc. IEEE Power Eng. Society General Meet.*, 2006, pp. 1-8.

[6] M. N. Marwali, J.-W. Jung, and A. Keyhani, "Control of distributed generation systemsPart II: Load sharing control," *IEEE Trans. Power Electron.*, vol. 19, no. 6, pp. 1551-1561, Nov. 2004.

[7] K. D. Brabandere, B. Bolsens, J. V. den Keybus, A. Woyte, J. Driesen, and R. Belmans, "A voltage and frequency droop control method for parallel inverters," *IEEE Trans. Power Electron.*, vol. 22, no. 4, pp. 1107-1115, Jul. 2007.

[8] E. Barklund, N. Pogaku, M. Prodanovic, C. Hernandez-Aramburo, and T. C. Green, "Energy management in autonomous Microgrid using stabilityconstrained droop control of inverters," *IEEE Trans. Power Electron.*, vol. 23, no. 5, pp. 2346-2352, Sep. 2008.

[9] D. De and V. Ramanarayanan, "Decentralized parallel operation of inverters sharing unbalanced and nonlinear loads," *IEEE Trans. Power Electron.*, vol. 25, no. 12, pp. 3015-3025, Dec. 2010.

[10] R. Majumder, B. Chaudhuri, A. Ghosh, R. Majumder, G. Ledwich and F. Zare, "Improvement of stability and load sharing in an autonomous Microgrid using supplementary droop control loop," Power and Energy Society General Meeting, 2010 IEEE , vol., no., pp. 25-29, July 2010.

[11] C.C. Chang, D. Gorinevsky and S. Lall, "Stability analysis of distributed power generation with droop inverters," *IEEE Trans. Power Systems*, vol.30, no.6, pp.3295-3303, Nov. 2015.

[12] Z. Miao, A. Domijan and L. Fan, "Investigation of Microgrids with both inverter interfaced and direct AC-Connected distributed energy resources," *IEEE Trans. Power Del.*, vol.26, no.3, pp.1634-1642, July 2011.

[13] A. Engler and N. Soultanis, "Droop control in LV-grids," *in Proc. IEEE Future Power Syst.*, Nov., 2005, pp. 1-6.

[14] M. Liserre, F. Blaabjerg, and S. Hansen, "Design and control of an LCL-filter-based three-phase active rectifier," *IEEE Trans. Ind. Appl.*, vol. 41, no. 5, Sep./Oct. 2005, pp. 1281-1291.

[15] B. Shi, G. Venkataramanan, and N. Sharma, "Design considerations for reactive elements and control parameters for three phase boost rectifiers," *in Proc. IEEE Electric Mach. Drives Conf.*, May 2005, pp. 1757-1764.

[16] Chia-Tse Lee, Chia-Chi Chu and Po-Tai Cheng, "A new droop control method for the autonomous operation of Distributed Energy Resource Interface Converters," *IEEE Trans. Power Electron.*, Vol. 28, No. 4, April 2013, pp. 1980-1993.

[17] E. Coelho, P. Cortizo, and P. Garcia, "Small-signal stability for parallelconnected inverters in stand-alone ac supply systems," *IEEE Trans. Ind. Appl.*, vol. 38, no. 2, pp. 533-542, Mar./Apr. 2002.

[18] L. Luo and S.V. Dhople, "Spatiotemporal model reduction of inverter-Based islanded Microgrids," *IEEE Trans. Energy Conversion*, vol.29, no.4, pp.823-832, Dec. 2014.

[19] N. Pogaku, N. Prodanovic, and T. Green, "Modeling, analysis and testing of autonoumous operation of an inverter-based Microgrid," *IEEE Trans. Power Electron.*, vol. 22, no. 2, pp. 613-625, Mar. 2007.

[20] Y. Mohamed and E. Saadany, "Adaptive decentralized droop controller to preserve power sharing stability of paralleled inverters in distributed generation Microgrids," *IEEE Trans. Power Electron.*, vol. 23, no. 6, pp. 2806-2816, Nov. 2008.

[21] S.V. Iyer, M.N. Belur, and M.C. Chandorkar, "A generalized computational method to determine stability of a multi-inverter Microgrid," *IEEE Trans. Power Electron.*, vol. 25, no. 9, pp. 2420-2432, Sep. 2010.

978-1-4799-8397-1/16/$31.00 © 2016 IEEE